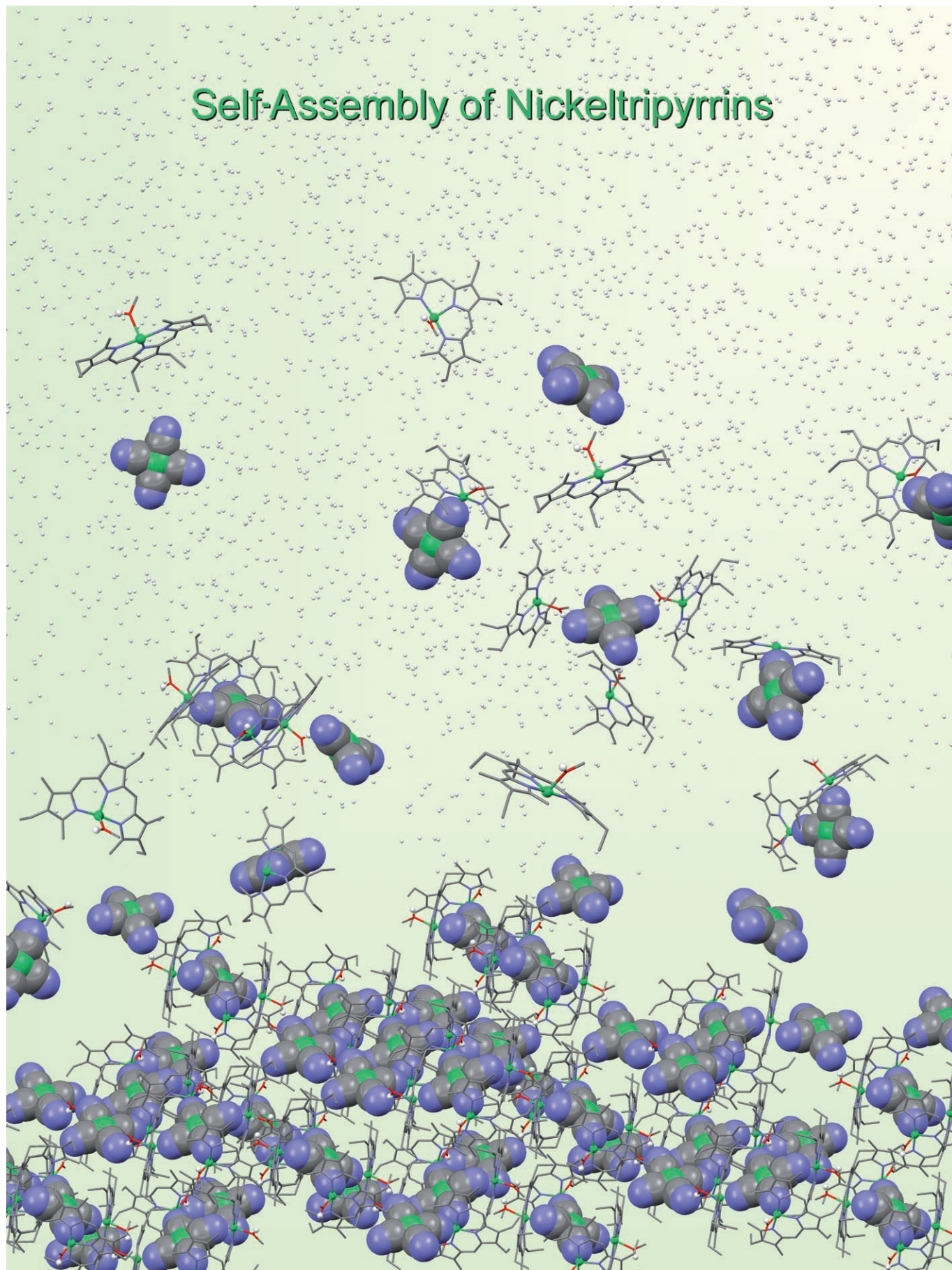


Self-Assembly of Nickeltripyrins



Pillars, Layers, Pores and Networks from Nickeltripyrins: A Porphyrin Fragment as a Versatile Building Block for the Construction of Supramolecular Assemblies

Martin Bröring,* Serguei Prikhodovski, Carsten D. Brandt, and Esther Cónsul Tejero^[a]

Abstract: Sterically hindered nickel-tripyrins [Ni(trpy)X] with different di-, tri- and tetradentate anions X have been prepared with the aim of finding coordination polymers formed by self-association. The syntheses were performed by simple ligand-exchange reactions and proceeded successfully with the pseudohalides CN⁻, OCN⁻, SCN⁻, SeCN⁻, N(CN)₂⁻ (dicyanoamido, dca) and C(CN)₃⁻ (tricyanomethanido, tcm), the cyanidometallates [Ag(CN)₂]⁻ and [Ni(CN)₄]²⁻ and the salicylate anion (sal⁻). X-ray crystallographic analyses

revealed that the complexes with cyano- and isocyanato ligands, as well as the compound with a salicylato ligand, are prototypes for structurally distinct monomeric species in the solid state, whereas one-dimensional coordination polymers or supramolecular three-dimensional networks are formed from all other combinations. The polymeric

compounds display a variety of individual pillar and network architectures with functionalised pores and clefts and with the Ni(trpy) fragments in different relative orientations. Hydrogen bonding and π stacking were found to be additional structure-directing effects, which increased the structural complexity of the system. The Ni(trpy) subunit has thus been proven to be a versatile building block for the construction of supramolecular assemblies and metal organic frameworks (MOFs) from pentacoordinate Ni^{II} ions.

Keywords: chain structures • nickel • porphyrinoids • supramolecular chemistry • tripyrrins

Introduction

The construction of one-, two- or three-dimensional coordination polymers through the self-assembly of transition-metal ions or complex fragments with polydentate ligands is a rapidly growing branch of modern coordination chemistry. Progress in this field has been widely reported over the last decade and numerous reviews on different aspects of supramolecular coordination polymers have been published.^[1–6] Much of this research was motivated by crystal engineering^[1,7–11] and the preparative access to new functional materials with potential applications in catalysis, photoluminescence, non-linear optics, gas storage (especially for dihydrogen), drug delivery and as single-chain magnets or conductors.^[2,6] The design of such systems demands suitable polydentate ligands that serve as bridging units between neighbouring metal centres. Pseudohalides like SCN⁻,

SeCN⁻, N(CN)₂⁻ (dicyanoamide, dca) and related species as well as cyanidometallates are of particular interest in this regard owing to their ability to coordinate to metal ions in different modes and numbers. By using bridging ligands from this group, one-, two- and three-dimensional assemblies with individual functionalities can be produced from many metal ions and complex fragments. The dimensionality of the product and the degree of oligo- and polymerisation depend critically on the type and nature of the bridging ligand, the steric influence and the basicity of the visitor ligand(s) and the charge, coordination number and geometry of the metal ion(s) used. Owing to this large number of critical parameters, however, the straightforward synthesis of coordination polymers with particular structural and/or functional features is still largely a matter of heuristic concepts.

Tripyrrins^[12–21] are short, open-chain oligopyrroles, the coordination properties^[22–24] of which we have studied as analogues to a series of ring-modified porphyrin variants.^[25–27] The most pronounced feature of α,ω -dimethyltripyrin ligands is the location of the methyl termini, which block one of the coordination sites of a central metal ion in the *N,N,N*-plane. Significant steric strain is thus produced in complexes with square-planar or octahedral coordination so that in general metallotripyrrins are not observed to adopt either of

[a] Prof. Dr. M. Bröring, Dr. S. Prikhodovski, Dr. C. D. Brandt, E. C. Tejero
 Fachbereich Chemie, Philipps-Universität Marburg
 Hans-Meerwein-Straße, 35043 Marburg (Germany)
 Fax: (+49)6421-282-5653
 E-mail: Martin.Broering@chemie.uni-marburg.de

these two important coordination geometries. As we have shown in the past, a transition-metal ion in a α,ω -dimethyl-tripyrin environment reacts either by severely tilting the additional ligand X or L away from the tripyrrolic plane or by pentacoordination (Figure 1). In the case of the Ni^{II} ion this behaviour has so far resulted in the exclusive formation of high-spin complexes.^[28,29]

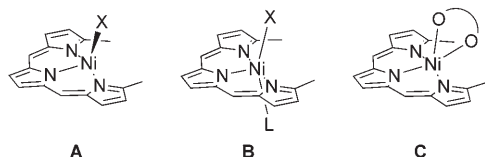
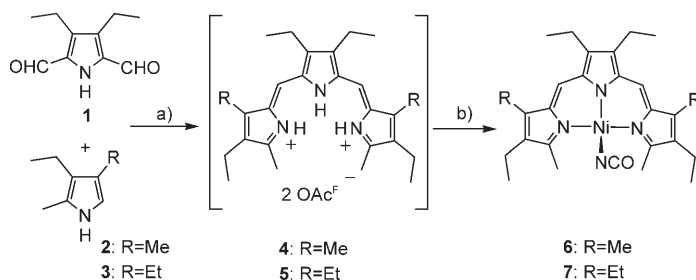


Figure 1. Generalised view of tetra- and pentacoordinate nickel(II)tripyrin structures.

In the α,ω -dimethyltripyrin environment the nickel(II) ion can employ two different modes of pentacoordination. Nitrate and oxalato species make use of type **C** coordination (Figure 1) in which both oxygen donor atoms of the external ligand bind from the same side of a slightly distorted tripyrrolic plane. Solvate complexes like the aquo species [Ni(trpy)Cl(OH₂)] on the other hand prefer a less strained coordination of type **B** with both additional donor centres bound to opposite sites of the tripyrrolic plane. This binding mode allows two or more Ni(trpy) fragments to be bridged in a linear fashion. In order to prepare such coordination oligo- and polymers we have attempted to combine the Ni(trpy) subunit with potential anionic bridging ligands from the pseudohalide, cyanidometallate and salicylate classes. Herein we report the results of this study.

Results and Discussion

Synthesis and properties of precursor species [Ni(trpy)(NCO)] **6 and **7**:** The synthesis of tripyrrolic complexes is a special challenge because it is complicated by the sensitivity of the trpy ligand towards nucleophiles. This property is unique for tripyrrins and bears only little resemblance to other oligopyrrolic systems.^[30] A typical procedure optimised to overcome this drawback is outlined in Scheme 1



Scheme 1. Synthesis of [Ni(trpy)(NCO)] complexes **6** and **7**. Reagents and conditions: a) TFA, reflux; b) Ni(OAc)₂·4H₂O, NaOAc, MeOH.

and involves the double condensation of the dialdehyde **1** with two equivalents of the α -non-substituted pyrrole **2** or **3** in boiling trifluoroacetic acid HOAc^F.^[24] Concomitant removal of the acidic solvent, treatment of the dark green, lustrous residue **4** or **5** with excess nickel acetate hydrate in methanol and silica filtration with dichloromethane/methanol as eluent yield dark green solutions. Upon addition of sodium cyanate, stable [Ni(trpy)(NCO)] complexes **6** and **7** form that can be isolated after recrystallisation in 43 and 55% yields, respectively.

Complexes **6** and **7** both dissolve easily in dichloromethane, pointing to their substantially monomeric character in solution. This was confirmed by solution susceptibility (performed by the Evans method^[31,32]) and ¹H NMR measurements, which clearly characterise the new complexes as the expected high-spin Ni^{II} species with effective magnetic moment (μ_{eff}) values of 3.1 ± 0.2 (**6**) and $3.0 \pm 0.2 \mu_{\text{B}}$ (**7**). The CN stretching frequencies for **6** and **7** ($\tilde{\nu} = 2208$ and 2210 cm^{-1}) are characteristic of terminal, non-bridging and N-bound isocyanates. Additional support for the monomeric nature of these complexes comes from the crystallographic study of **7** (see below). Because **6** and **7** proved quite stable in solution they were chosen for solvent addition studies and as precursors for further transformations.

Solvent addition to [Ni(trpy)(NCO)] **7** was studied by ¹H NMR and UV/Vis spectroscopy in order to investigate association and possible oligomerisation processes in solution. ¹H NMR spectra were recorded for samples in CD₂Cl₂, C₆D₆, [D₆]acetone, [D₆]DMSO and CD₃OD at approximate concentrations of $2 \times 10^{-2} \text{ mol L}^{-1}$. Significant changes in the spectra upon association of a fifth ligand were observed for the nickel chelate. Representative spectra of **7** in different solvents are given in Figure 2. The spectra of **7** in non-donor solvents like CD₂Cl₂ or C₆D₆ are typical of four coordinate [Ni^{II}(trpy)] species.^[28] The formation of solvent adducts in deuterated DMSO and methanol, as well as in [D₆]acetone, is indicated by large shifts of some of the resonance signals. These changes are particularly pronounced for the proton signals of the terminal methyl groups CH₃^{term}, which are shifted by about $\delta = 40$ ppm to a higher field upon association with a fifth donor. In addition, a small but characteristic high-field shift is observed for the signals of the *meso*-situated protons H_{meso}. Notwithstanding pseudocontact shifts, the high-field shifts of the CH₃^{term} and H_{meso} signals (positive contact shifts) are indicative of a preferential π mechanism for spin delocalisation in the pentacoordinate complexes of geometry **B**, whereas spin delocalisation (with negative contact shifts) in distorted tetracoordinate species seems dominated by the σ mechanism.^[33]

Whereas the spectra of pentacoordinate donor adducts [Ni(trpy)(L)X] are typically slightly different for different anionic ligands X,^[28] the spectra of the complexes in CD₃OD and in [D₆]DMSO are always identical for one Ni(trpy) fragment. We attribute this finding to the way in which neutral [Ni(trpy)(L)X] species are formed with most donor solvents, whereas in methanol as well as in DMSO charge separation takes place, resulting in cationic [Ni-

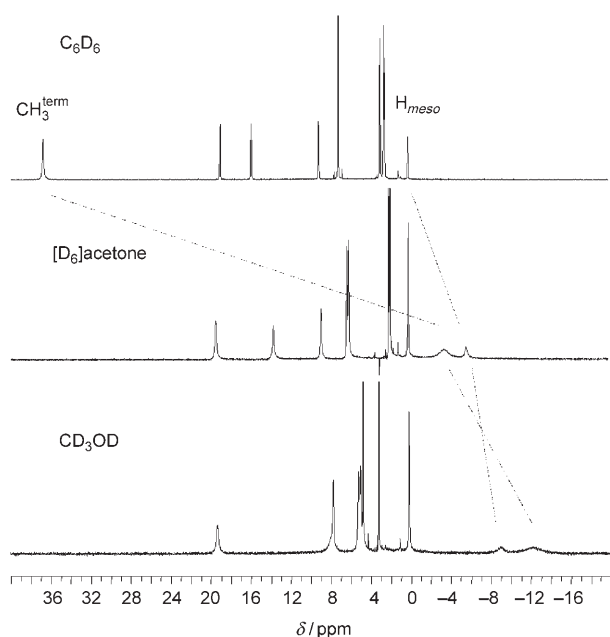


Figure 2. Representative ^1H NMR spectra of $[\text{Ni}(\text{trpy})(\text{NCO})]$ **7** in solvents with different donating abilities.

$(\text{trpy})(\text{L})_2]^+$ species and solvated anions X^- . The pronounced tendency for nickel(II)tripyrins to form pentacoordinate complexes has been discussed before and is an expression of their increased reactivity relative to, for example, low-spin nickel(II) porphyrins. The formation of hexacoordinate species, however, which is typical for other high-spin nickel(II) complexes, cannot be observed for steric reasons.

UV/Vis spectra were measured at room temperature in dichloromethane, acetone and methanol at concentrations of approximately $10^{-6} \text{ mol L}^{-1}$. $[\text{Ni}(\text{trpy})(\text{NCO})]$ **7** exhibits characteristic and strong absorptions between $\lambda=300$ and 800 nm that can be assigned to ligand $\pi-\pi^*$ transitions in all cases (Figure 3). In analogy with the porphyrins, one intense absorption is present in the high frequency part of the spectra at about $\lambda=350 \text{ nm}$ and a number of overlapping bands

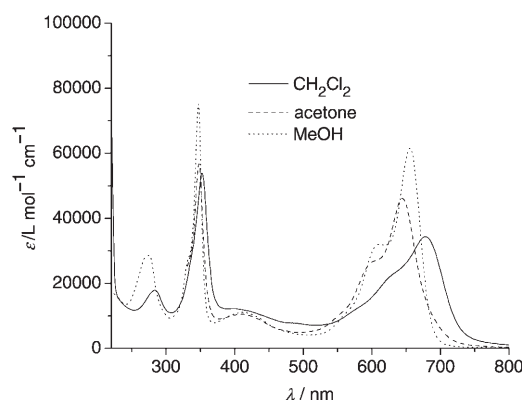
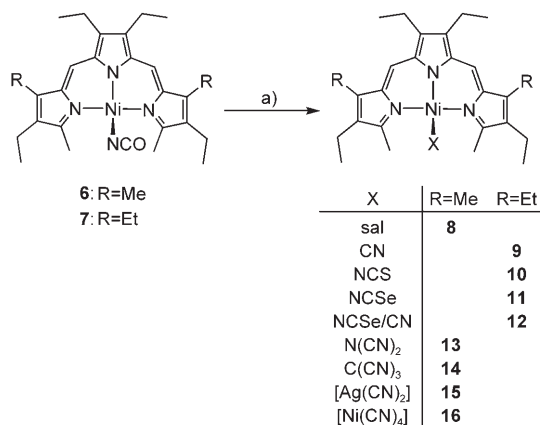


Figure 3. UV/Vis spectra of $[\text{Ni}(\text{trpy})(\text{NCO})]$ **7** in dichloromethane, acetone and methanol.

appear between $\lambda=500$ and 800 nm . The transition from a tetracoordinate species to a pentacoordinate one is accompanied by a bathochromic shift and an increase in the intensity of the low energy bands. By using these observations as criteria for donor association, UV/Vis spectra as well as ^1H NMR spectra can be used to characterise the oligomerisation processes of $[\text{Ni}(\text{trpy})\text{X}]$ species in solution.

Ligand exchange on 6 and 7—Monomer versus polymer formation: The introduction of a potentially bridging salicylate, pseudohalide or cyanidometallate ligand into the metallotripyrin system can be performed simply by extraction of an ethereal solution of **6** or **7** with an aqueous solution of excess salt NaX or KX (Scheme 2). The desired $[\text{Ni}(\text{trpy})\text{X}]$ complexes form in all cases except with the cyanido deriva-



Scheme 2. Reagents and conditions: a) MX ($\text{M}=\text{Na}, \text{K}$), $\text{Et}_2\text{O}/\text{H}_2\text{O}$.

tives, with which isolable compounds were obtained only if the cyanide ion was applied in a very low concentration. Nine new complexes **8–16** were isolated, seven of which could be analysed crystallographically. All the new compounds were of analytical purity and were further characterised by using NMR, UV/Vis and mass spectrometry. ^1H NMR spectra of the salicylato and cyanido derivatives **8** and **9** (the only diamagnetic compound in the series) were recorded in CD_2Cl_2 as were the slightly soluble isothiocyanato **10** and isoselenocyanato complexes **11** and **12**. Compounds **13–16** proved insufficiently soluble in dichloromethane. The ^1H NMR spectra of these species in $[\text{D}_6]\text{DMSO}$ are essentially identical, which indicated complete dissociation and the formation of $[\text{Ni}(\text{trpy})([\text{D}_6]\text{dmsO})_2]^+$ ions throughout. The mass spectra of **8–16** are dominated by strong signals originating from the cationic $\text{Ni}(\text{trpy})^+$ fragments and anionic co-ligands could not be recorded even for **9**.

The soluble isocyanato, salicylato and cyanido complexes **7**, **8** and **9** crystallise as monomers by slow diffusion of pentane into the respective solutions in dichloromethane at -60°C . Figure 4 shows the results of the single-crystal X-ray diffraction studies. Additional details of the structure solutions and refinements are summarised in Table 1.

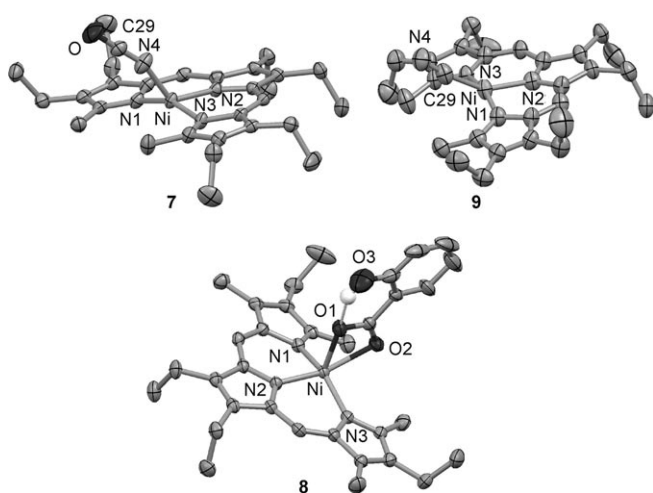


Figure 4. Molecular structures of [Ni(trpy)(NCO)] **7**, [Ni(trpy)(sal)] **8** and [Ni(trpy)(CN)] **9** in the solid state. Selected bond lengths [Å] and angles [°]: **7**: Ni–N1 1.9815(15), Ni–N2 1.9384(14), Ni–N3 1.9758(14), Ni–N4 1.9353(17), N4–C29 1.144(2), C29–O 1.203(2); N1–Ni–N2 93.34(6), N1–Ni–N3 158.39(6), N1–Ni–N4 97.55(7), N2–Ni–N3 92.96(6), N2–Ni–N4 124.39(7), N3–Ni–N4 95.87(7), Ni–N4–C29 159.55(18), N4–C29–O 178.5(2); **8**: Ni–N1 2.000(2), Ni–N2 1.970(2), Ni–N3 2.007(2), Ni–O1 2.0729(19), Ni–O2 2.2057(19); N1–Ni–N2 91.92(9), N1–Ni–N3 151.48(8), N1–Ni–O1 101.53(9), N1–Ni–O2 92.31(8), N2–Ni–N3 92.01(9), N2–Ni–O1 97.88(8), N2–Ni–O2 158.92(8), N3–Ni–O1 105.87(9), N3–Ni–O2 94.06(8), O1–Ni–O2 61.05(7); **9**: Ni–N1 1.908(4), Ni–N2 1.912(3), Ni–N3 1.908(4), Ni–C29 1.849(4), C29–N4 1.181(6); N1–Ni–N2 93.13(15), N1–Ni–N3 163.08(16), N1–Ni–C29 91.28(18), N2–Ni–N3 92.87(14), N2–Ni–C29 149.24(18), N3–Ni–C29 91.64(18), Ni–C29–N4 169.4(4). Thermal ellipsoids are set at the 50% probability level. Hydrogen atoms have been omitted for clarity.

Complexes **7**, **8** and **9** can be regarded as prototypical examples of type **A** high-spin, type **C** high-spin and type **A** low-spin Ni^{II}–terpyrins, respectively. The bond lengths found within the coordination polyhedra develop as expect-

ed in the order **9** < **7** < **8**. In addition, the low-spin character of **9** is indicated by the planarity of the coordination environment, as quantified by the reduced tilt of the external ligand binding of approximately 25° with respect to **7**.

Why do **8** and **9** only form monomeric structures? The free coordination site at the Ni^{II} ion of the salicylate **8** opposite O1 seems to be unavailable for a sixth ligand owing to the severe doming of the metal ion of 0.459 Å from the terpyridin N₃ plane. In addition to this it appears necessary to rotate the phenyl ring away prior to forming a polymer with type **B** coordination subunits. The unfavourable aryl ring conformation, however, is strengthened by an intramolecular hydrogen bond, and the strain from the four-membered chelate ring seems to be too small to overcome this barrier. The Ni^{II} ion in the low-spin compound **9**, on the other hand, should be electronically saturated with four ligands. The steric interference of the cyanido ligand with the terminal methyl groups is evidently not so severe as to favour the binding of a fifth donor atom accompanied by a change in spin state. Steric reasons relating to the shortness of a potential cyanido bridge might also play a role.

Association phenomena were observed with the thiocyanate and selenocyanate ligands in compounds **10** and **11**. Unlike cyanate, the thiocyanate ion has often been reported as a suitable bridging ligand in coordination polymers.^[34,35] The same is true of the homologous selenocyanate, although reports are rather rare.^[35,36] In the solid state, the compounds [Ni(trpy)(NCS)] **10** and [Ni(trpy)(NCSe)] **11** show CN stretching frequencies at $\tilde{\nu}$ = 2104 and 2112 cm⁻¹, respectively, which is an indication of μ -(N,S/Se) coordination.^[37] Whereas the UV/Vis spectra of **10** and **11** in very dilute solutions are in accordance with basically monomeric species, the ¹H NMR spectra interestingly show a signal pattern related to that of **7**, but with strongly reduced paramagnetic

Table 1. Crystal data and structure refinement for compounds **7**–**10**, **12**–**14** and **16**.^[a]

	7	8	9	10	12 ·CH ₂ Cl ₂	13	14	16'
formula	C ₂₉ H ₃₈ N ₄ NiO	C ₃₃ H ₃₉ N ₃ NiO ₃	C ₂₉ H ₃₈ N ₄ Ni	C ₂₉ H ₃₈ N ₄ NiS	C ₅₉ H ₇₈ Cl ₂ N ₈ Ni ₂ Se	C ₂₈ H ₃₄ N ₆ Ni	C ₃₀ H ₃₄ N ₆ Ni	C ₁₁₆ H ₁₅₂ N ₂₀ Ni ₆ O ₄
<i>M</i> _r	517.32	584.36	501.32	533.40	1166.58	513.32	537.34	2242.84
system	triclinic	triclinic	triclinic	monoclinic	triclinic	monoclinic	monoclinic	orthorhombic
space group	<i>P</i> $\bar{1}$	<i>P</i> $\bar{1}$	<i>P</i> $\bar{1}$	<i>P</i> 2 ₁ / <i>c</i>	<i>P</i> $\bar{1}$	<i>P</i> 2 ₁	<i>P</i> 2 ₁ / <i>n</i>	<i>C</i> 2/ <i>c</i>
<i>a</i> [Å]	11.0457(8)	9.7458(9)	10.9952(16)	13.5213(6)	13.2714(19)	12.9401(8)	8.4291(8)	28.274(18)
<i>b</i> [Å]	11.0884(8)	12.7269(15)	11.0470(16)	19.5377(9)	15.274(2)	15.7676(10)	29.267(3)	14.537(11)
<i>c</i> [Å]	11.8603(9)	13.5853(14)	11.9836(15)	11.3302(5)	15.587(2)	13.8538(9)	11.4946(11)	27.809(8)
α [°]	93.826(1)	112.239(12)	95.370(17)	90	84.690(17)	90	90	90
β [°]	112.637(1)	101.897(11)	114.119(15)	104.545(10)	77.164(16)	104.3800(10)	105.303(2)	90
γ [°]	90.987(1)	98.128(13)	91.177(18)	90	68.488(16)	90	90	90
<i>Z</i>	2	2	2	4	4	4	4	8
ρ _{calcd} [g cm ⁻³]	1.286	1.311	1.261	1.223	1.352	1.245	1.305	1.303
size [mm]	0.30 × 0.30 × 0.20	0.21 × 0.19 × 0.15	0.24 × 0.19 × 0.13	0.22 × 0.22 × 0.19	0.21 × 0.12 × 0.04	0.31 × 0.30 × 0.14	0.17 × 0.10 × 0.03	0.25 × 0.21 × 0.15
<i>T</i> [K]	173(2)	193(2)	193(2)	173(2)	193(2)	153(2)	193(2)	193(2)
data collection	ω scan	φ scan	φ scan	ω scan	φ scan	ω scan	ω scan	φ scan
θ range [°]	1.84–25.00	2.20–25.92	1.87–25.94	1.56–25.00	1.95–25.65	2.32–27.31	1.96–25.35	1.74–26.09
measured refl.	25 671	14 300	13 045	27 423	25 962	44 182	27 043	42 588
indep. refl. ^[b]	4460	5342	2356	5082	9491	11 182	5002	10 721
abs. coefficient	0.754	0.693	0.758	0.765	1.430	0.735	0.739	1.028
solution ^[c]	direct	Patterson	Patterson	direct	Patterson	direct	Patterson	direct
final <i>R</i> ₁ value	0.0310	0.0413	0.0534	0.0415	0.0823	0.0326	0.0610	0.0310

[a] Data collections were performed at 153 (**13**), 173 (**7**, **10**) or 193 K on an IPDS1 (**8**, **12**, **16'**), IPDS2 (**9**) or Bruker Smart Apex diffractometer with graphite-monochromated Cu_{K α} radiation. [b] $I > 2\sigma(I)$. [c] All structures were solved using SHELXS^[41] and refined with SHELXL.^[42]

shifts (Figure 5). In fact, Evans measurements of the new species provide μ_{eff} values of only 2.2 ± 0.2 and $2.1 \pm 0.2 \mu_{\text{B}}$ at 295 K, respectively. We attribute this finding to the beginning of the oligomerisation process of **10** and **11** in solution, allowing weak antiferromagnetic exchange between paramagnetic Ni^{II} ions in the oligomeric arrangements.

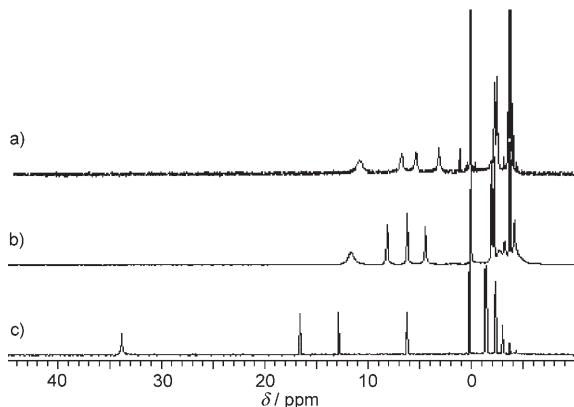


Figure 5. ^1H NMR spectra (295 K, CD_2Cl_2) of a) **7**, b) **10** and c) **11**.

Single crystals of $[\text{Ni}(\text{trpy})(\text{NCS})]$ **10** were grown by slow diffusion of *n*-hexane into a solution of **10** in dichloromethane at -60°C . The results of the X-ray diffraction study given in Figures 6 and 7 show the formation of a one-dimensional coordination polymer from $\mu(\text{N},\text{S})$ -thiocyanate ions and $\text{Ni}(\text{trpy})$ fragments of type **B**. The pentacoordinate monomeric unit is characterised by $\text{Ni}-\text{N}_{\text{trpy}}$ bond lengths of 1.97–2.03 Å, an almost planar $\text{Ni}(\text{trpy})$ fragment and a N4–Ni–S angle of 142° . The Ni–S bond in solid **10** is as long as 2.48 Å and appears rather weak, as expected for the coordination of a hard Ni^{2+} ion with a soft sulfur donor. The monomeric units are arranged in linear chains with intra-

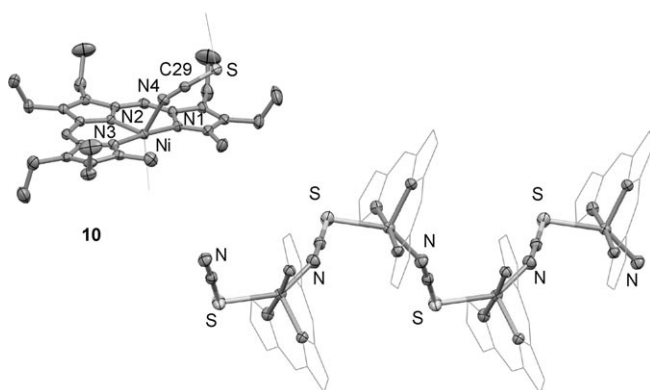


Figure 6. Structure of the monomeric subunit and details of the chain structure of polymeric $[\text{Ni}(\text{trpy})(\text{NCS})]$ **10** (alkyl side chains removed). Selected bond lengths [Å] and angles [$^\circ$]: Ni–N1 2.0254(18), Ni–N2 1.9769(18), Ni–N3 2.0092(18), Ni–N4 2.061(2), Ni–S 2.4830(7), N4–C29 1.154(3), C29–S 1.654(2); N1–Ni–N2 92.16(7), N1–Ni–N3 174.47(8), N1–Ni–N4 87.45(8), N1–Ni–S 86.60(6), N2–Ni–N3 93.14(7), N2–Ni–N4 114.11(8), N2–Ni–S 102.96(6), N3–Ni–N4 91.84(8), N3–Ni–S 90.67(6), N4–Ni–S 142.63(6), Ni–N4–C29 151.7(2), N4–C29–S 176.9(2), C29–S–Ni 106.76(8). Thermal ellipsoids are set at the 50% probability level. Hydrogen atoms have been omitted for clarity.

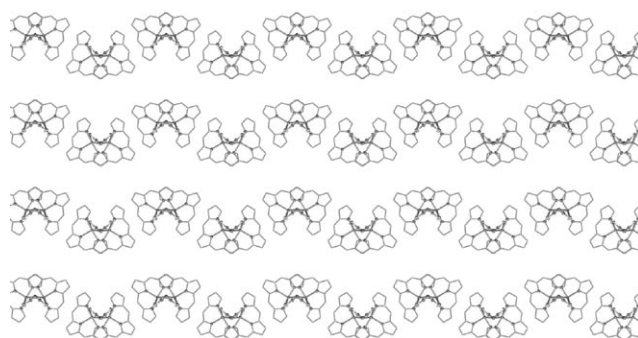


Figure 7. Sheet structure formed by weakly interacting helical pillars of **10** (view along the crystallographic *c* axis; alkyl chains have been omitted for clarity).

chain Ni···Ni distances of 6.236 Å. As a consequence of the steric influence of the bridging thiocyanato ligand, the adjacent $\text{Ni}(\text{trpy})$ planes are tilted by 38.8° and rotated by 113.3° so that the $(\text{Ni}-\text{N}-\text{C}-\text{S})_n$ chains form helices. This special arrangement allows tight intrastrand packing of the monomers with minimum distances between the methylene carbon atoms of one unit and the sp^2 system of the next of 3.366 Å and without losing the rather weak Ni–S coordination.

In the crystal lattice the helical polymer chains form pillars with several interstrand alkyl– π interactions as close as 3.35 Å. The resulting arrangement can be addressed as a zig-zag sheet structure formed from layered pillars (Figure 7). The closest interstrand Ni···Ni distance was found to be 7.75 Å.

A quite intriguing and unexpected facet of the solid-state structure of **10** comes from a comparison with the known structure of $[\text{Ni}(\text{trpy})\text{Cl}(\text{H}_2\text{O})]$ ^[28] in which hydrogen bonds result in the formation of a one-dimensional polymeric chain (Figure 8). The arrangement of the $\text{Ni}(\text{trpy})$ fragments is isotypical in both cases, albeit the bridging unit is linear and covalently bound in **10**, but tilted and hydrogen-bonded in the chlorido complex. The relative orientation of the $\text{Ni}(\text{trpy})$ units in the latter is characterised by a tilt of 37.6° and a torsion angle of 111.0° , with the shortest Ni···Ni distances for the chlorido derivative being 6.374 Å (intrastrand) and 7.415 Å (interstrand). Even the intra- and interstrand

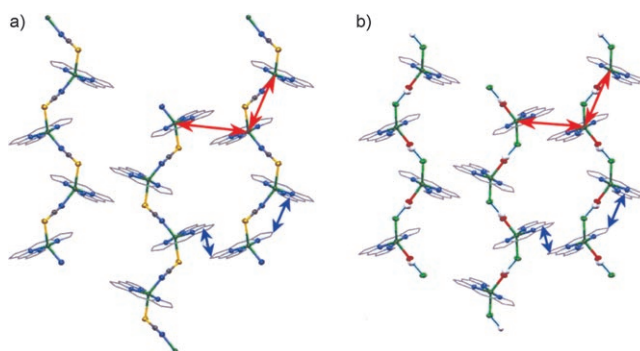
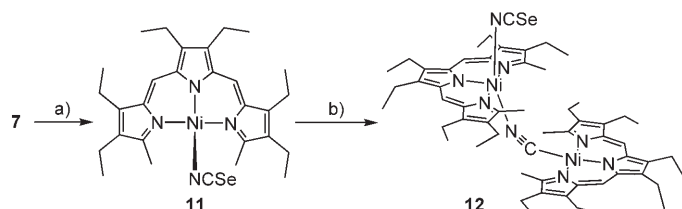


Figure 8. Equivalent arrangements of the nearest-neighbour pillars in a) solid $[\text{Ni}(\text{trpy})(\text{NCS})]$ **10** and b) $[\text{Ni}(\text{trpy})\text{Cl}(\text{H}_2\text{O})]$. The arrows indicate the sites of closest intra- and interstrand Ni···Ni- and methylene– π distances, respectively.

methylene- π interactions are of comparable size, the shortest distances being 3.46 and 3.38 Å, respectively, for [Ni(trpy)Cl(H₂O)]. The tight packing of the Ni(trpy) motifs seems to govern the polymeric nickeltripyrin crystal structures when small bridges are employed.

Attempts to crystallise the selenocyanato analogue **11**, which was prepared from **7** and potassium selenocyanate in the same fashion as **10**, led to the slow decomposition of the material with concomitant precipitation of red selenium (Scheme 3). After eight weeks as a solution in dichlorome-



Scheme 3. Reagents and conditions: a) KNCSe, Et₂O/H₂O; b) CH₂Cl₂, 2 months.

thane/*n*-hexane at 4 °C dark violet crystals formed from the decomposition product **12**·CH₂Cl₂. The dinuclear structure of **12** was determined by single-crystal X-ray diffraction studies (Figure 9) and was confirmed analytically.

Complex **12** is composed of two Ni(trpy) subunits with one high-spin and one low-spin nickel(II) ion. Comparison with [Ni(trpy)(CN)] **9** and [Ni(trpy)(NCS)]_n **10** reveals almost prototypical measurements for both subunits of **12** (see the table in Figure 9). All major differences are related

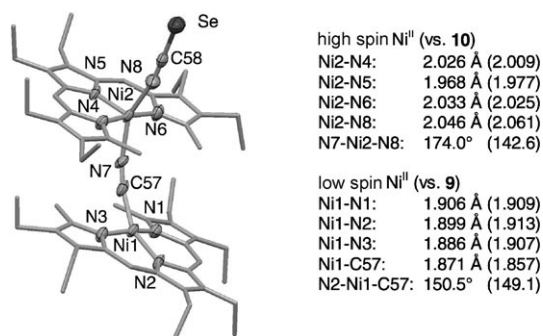


Figure 9. Molecular structure of the dinuclear complex **12** (hydrogen atoms and disordered dichloromethane molecule have been omitted for clarity). Selected data for both Ni(trpy) subunits and a comparison with [Ni(trpy)(CN)] **9** and [Ni(trpy)(NCS)]_n **10** structures are shown. Thermal ellipsoids are set at the 50% probability level.

to the bridging character of the cyanido ligand; as expected the CN bond is shortened by 0.042 Å and the Ni1-C57 bond elongated by 0.024 Å relative to **9**. The N7-Ni2-N8 angle of the high-spin Ni(trpy) subunit is found to be 174.0°, which indicates a transition from a distorted trigonal-bipyramidal coordination environment in **10** to a square-pyramidal one. We assume that this transition is mainly induced by steric effects as the low-spin Ni(trpy) subunit gains more distance from the high-spin Ni(trpy) plane through steeper binding of the short cyanido ligand. The high- and low-spin Ni(trpy) fragments of **12** are arranged in an unstrained and almost

coplanar fashion. The tilt between the mean N₃ planes is only 7.4° with a torsion angle of 177.3°. This leads to contacts between the subunits of not less than 4.121 Å and a Ni...Ni distance of 4.905 Å.

The binding mode of the selenocyanato and cyanido ligands in **12** can also be concluded from the IR spectra as a shift of the CN stretching bands to higher wavenumbers is expected upon bridging.^[37] In fact, the transition of the selenocyanate from a bridging binding mode in **11** to terminal bonding in **12** is accompanied by a shift of the $\tilde{\nu}_{\text{CN}}$ band from 2113 to 2086 cm⁻¹. The cyanido ligand also follows this general trend as it induces stretching vibrations for **12** at 2153 and 2174 cm⁻¹ as compared with the band at 2117 cm⁻¹ observed for the monomer **9**. This example underlines the importance of IR spectra in determining the degree of association in the solid state.

An important conclusion from the above examples is that the CN unit provides optimum binding capabilities for nickeltripyrins. Therefore it can be predicted that anionic X(CN)_n-like bridges should be the best choice when forming coordination polymers from Ni(trpy) subunits. Dicyanoamide (dca), tricyanomethanide (tcm) and many cyanidometallates [M(CN)_n]^{m-} belong to this class of anion. They are used widely in the preparation of coordination polymers and in the field of crystal engineering as they provide three important features: 1) a large number of different possible binding and bridging modes, 2) larger distances between the metals necessary for pores and clefts and 3) additional functionality as employed, for example, in the bricks-and-mortar approach.^[38]

The treatment of [Ni(trpy)(NCO)] **6** with sodium dicyanoamide or potassium tricyanomethanide^[39] under standard conditions resulted in the immediate formation of insoluble products that could be isolated simply by filtration. IR spectroscopic investigations showed CN stretching bands at 2314 ($\tilde{\nu}_s + \tilde{\nu}_{\text{as}}$), 2251 ($\tilde{\nu}_{\text{as}}$) and 2185 cm⁻¹ ($\tilde{\nu}_s$) for the dca derivative **13** and at 2233 ($\tilde{\nu}_s + \tilde{\nu}_{\text{as}}$) and 2176 cm⁻¹ ($\tilde{\nu}_s$) for the tcm complex **14**. For **13** the high wavenumber of the ($\tilde{\nu}_s + \tilde{\nu}_{\text{as}}$) band is indicative of a 1,5 binding mode for the dca ligand and thus for the formation of a one-dimensional polymeric chain structure. The vibrational data obtained for the tcm derivative is inconclusive. The negligible solubility, however, clearly points to the presence of a coordination polymer also for **14**. Single crystals of **13** and **14** were obtained by layering solutions in methanol with toluene and allowing slow diffusion at 4 °C. The results of the X-ray crystallographic investigations are shown in Figure 10. The two new compounds crystallise in the linear arrangement anticipated for Ni(trpy) units. The tcm derivative **14** is composed of uniform monomers. The polymer chain formed from the dca complex **13** contains two very similar monomeric units Ni1(trpy) and Ni2(trpy) of which only Ni1(trpy) will be discussed further.

The monomeric subunits of **13** and **14** show structural parameters typical of type **B** high-spin Ni^{II} species. Unlike before, however, the binding between the nickel ion and the two external donors is now of comparable strength. The dca and tcm bridges lead to large Ni...Ni separations of 8.434

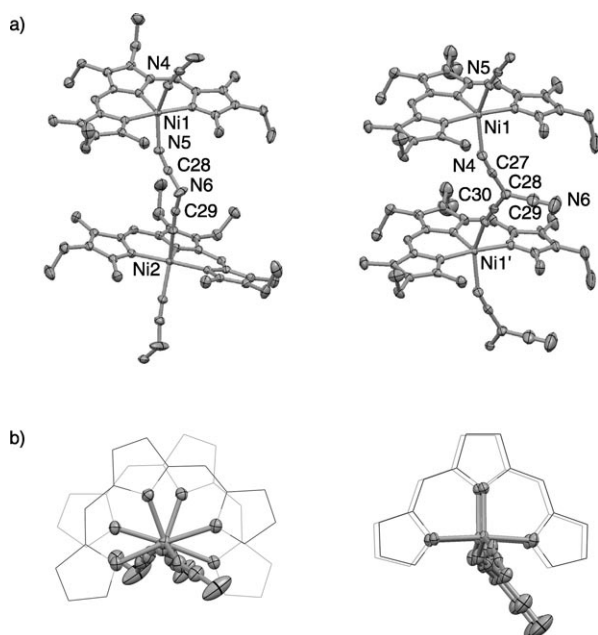


Figure 10. a) Structures of one-dimensional polymeric $[\text{Ni}(\text{trpy})(\text{dca})]$ **13** (left) and $[\text{Ni}(\text{trpy})(\text{tcm})]$ **14** (right) in the solid state and b) view along the Ni–Ni axes of **13** (left) and **14** (right; alkyl side chains removed). Selected bond lengths [Å] and angles [°]: **13**: Ni1–N1 2.0284(18), Ni1–N2 1.9689(18), Ni1–N3 2.0395(18), Ni1–N4 2.0592(18), Ni1–N5 2.0636(18), N5–C28 1.147(3), C28–N6 1.305(3); N4–Ni1–N5 147.53(8), Ni1–N5–C28 155.07(18), N5–C28–N6 171.8(2), C28–N6–C29 124.5(2); **14**: Ni1–N1 2.015(3), Ni1–N2 1.957(3), Ni1–N3 2.013(3), Ni1–N4 2.120(3), Ni1–N5 2.072(3), N4–C27 1.136(5), C27–C28 1.403(5), C28–C29 1.406(6), C29–N6 1.145(5); N4–Ni1–N5 146.10(13), Ni1–N4–C27 154.2(3), N4–C27–C28 176.4(4), C27–C28–C29 119.7(3), C27–C28–C30 121.4(3). Thermal ellipsoids are set at the 50% probability level. Hydrogen atoms have been omitted for clarity.

and 8.429 Å, respectively, and the tripyrrolic ligands of adjacent Ni(trpy) subunits are separated now by as much as 7.67 (13) and 8.32 Å (14). The Ni(trpy) planes in the tcm derivative 14 are arranged in a coplanar fashion and without any torsion, whereas in 13 a tilt of 10.1° and a torsion angle of 38.6° is observed. This difference can be explained by the steric influence of the third, non-coordinating cyano group of 14 Figure 10b.

The differences between the intrastrand structures of 13 and 14 markedly influence the relative arrangement of the pillars (Figure 11). The empty space between adjacent Ni(trpy) planes in a single chain of 13 is partially filled by two nearby pillars that come very close and whose Ni(trpy) units interdigitate at interstrand π – π distances of about 3.40 Å. As the next pillars are significantly further away a layered pillar structure results. Interestingly, the divalent central nitrogen atoms of the dca bridges are oriented towards the gaps between these layers, thus producing a functionalised cleft. Complex 14 instead forms a structure with almost isolated polymer chains in which six pillars arrange to form a trapezoid pore with dimensions of about 6.2 × 4.7 Å. The non-coordinated cyano group of two of these pillars point directly into this pore, resulting in functionalisation of the pore with N...N distances of 5.769 Å.

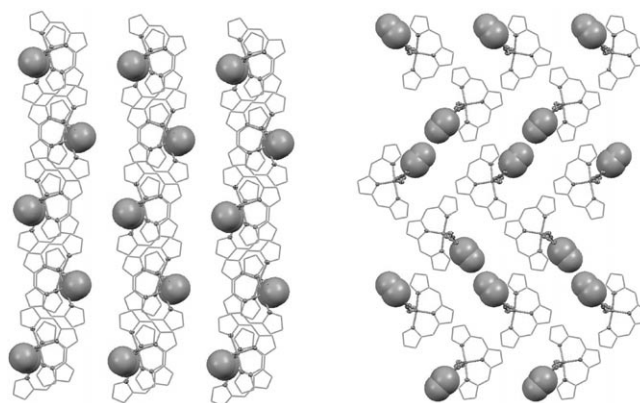


Figure 11. Views along the chains of **13** and **14**. CN functionalisation of clefts and pores formed by the different three-dimensional arrangements of the pillars of one-dimensional polymeric $[\text{Ni}(\text{trpy})(\text{dca})]$ **13** (left) and $[\text{Ni}(\text{trpy})(\text{tcm})]$ **14** (right), respectively.

The advent of functionalised inner surfaces within the Ni(trpy)-based coordination polymers tempted us to investigate metal-containing dicyanidoargentate $[\text{Ag}(\text{CN})_2]^-$ and tetracyanidonickolate $[\text{Ni}(\text{CN})_4]^{2-}$ anions as potential bridging ligands. Treatment of 6 with sodium dicyanidoargentate resulted in an insoluble product 15 that exhibits a single CN vibration at 2172 cm^{-1} . Relative to the free $[\text{Ag}(\text{CN})_2]^-$ ion this band is blueshifted by 37 cm^{-1} , which indicates the formation of a polymer. The use of tetracyanidonickolate as the bridging unit also results in the immediate precipitation of a product 16 with a single CN stretching frequency at 2155 cm^{-1} . Again, this value is blueshifted with respect to the free dianion by 27 cm^{-1} . Neither compound could be crystallised in their original form. Whereas only tiny needles could be obtained from 15, 16 slowly crystallised as the methanol adduct 16' from a solution in methanol/toluene. The results of the X-ray crystallographic analysis of these crystals are given in Figures 12, 13 and 14. Selected structural data are summarised in Table 2.

Complex 16' contains two slightly different monocationic subunits $[\text{Ni}1(\text{trpy})(\text{MeOH})]^+$ and $[\text{Ni}3(\text{trpy})(\text{MeOH})]^+$ of type B that display O–Ni–N_{CN} angles of 145.82(8) and 146.78(8)°. Two of each of these fragments coordinate to one $[\text{Ni}2(\text{CN})_4]^{2-}$ dianion and encapsulate it with Ni2...Ni1 and Ni2...Ni3 distances of 5.012(4) and 4.990(4) Å, respectively. Owing to the bridging binding mode of the cyanido ligands the CN bonds are as short as 1.154(3) and 1.146(3) Å. The result is a pentanuclear Ni₅ capsule dication with five coplanar nickel(II) ions and four peripheral methanol ligands (Figure 12).

The crystal structure of 16' is built from these dicationic Ni₅ capsules and additional $[\text{Ni}4(\text{CN})_4]^{2-}$ units for charge compensation. Ions and counterions form hydrogen bonds between the methanol and cyanido ligands with O...N distances of 2.799(4) and 2.756(4) Å (Figure 13b), resulting in a second set of short Ni4...Ni1 and Ni4...Ni3 distances of 7.174(5) and 6.948(5) Å, respectively.^[40] The CN bond lengths in the anionic moiety are 1.152(4) and 1.162(4) Å, slightly shorter than those in the dicationic Ni₅ capsule.

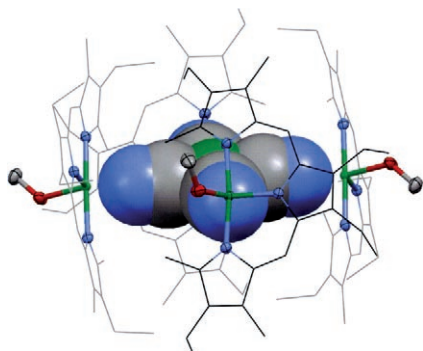


Figure 12. Encapsulation of one $[\text{Ni}(\text{CN})_4]^{2-}$ dianion by four $[\text{Ni}(\text{trpy})(\text{MeOH})]$ fragments and formation of a Ni_5 capsule (hydrogen atoms have been omitted).

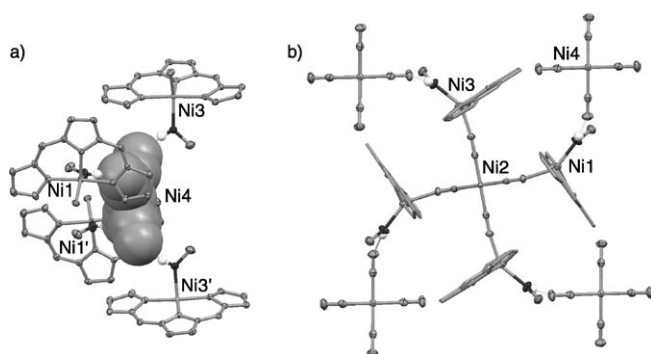


Figure 13. a) Distorted tetrahedral arrangement of the quadruply hydrogen-bonded $[\text{Ni}(\text{CN})_4]^{2-}$ dianion connecting four Ni_5 capsules. b) Connectivity of the hydrogen-bonded $[\text{Ni}(\text{CN})_4]^{2-}$ units at one Ni_5 capsule. Thermal ellipsoids are set at the 50% probability level. Carbon-bound hydrogen atoms and tripyrrin alkyl groups have been omitted for clarity.

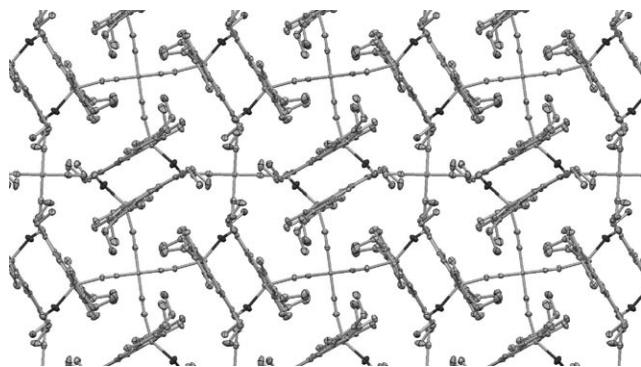


Figure 14. Tetranodal three-dimensional network structure of $\mathbf{16'}$ (view along the crystallographic b axis; hydrogen atoms have been omitted for clarity).

The higher flexibility of hydrogen versus coordinative binding results in Ni_5 capsules that are alternately arranged 2.764 Å above and below the mean plane of the hydrogen-bonded $[\text{Ni}(\text{CN})_4]^{2-}$ dianion (measured from the adjacent Ni^{II} centres), thus forming a flattened tetrahedral substructure (Figure 13a). This strong deviation from planarity, which is imposed by the low-spin Ni^{II} ions, explains why a

Table 2. Selected bond lengths [Å] and angles [°] for the different coordination environments of the nickel(II) ion in $\mathbf{16'}$.

	Ni1	Ni3	Ni2	Ni4
Ni–D1 ^[a]	2.004(2)	2.004(2)	1.877(3)	1.877(3)
Ni–D2	1.962(2)	1.9779(18)	1.849(3)	1.869(3)
Ni–D3	2.011(2)	2.009(2)	1.877(3)	1.877(3)
Ni–D4	2.079(2)	2.008(2)	1.849(3)	1.869(3)
Ni–D5	2.153(2)	2.098(2)	–	–
D1–Ni–D2	93.18(8)	92.89(8)	90.57(10)	88.83(11)
D1–Ni–D3	173.86(8)	173.51(8)	180.00(15)	169.26(15)
D1–Ni–D4	94.59(8)	89.61(8)	89.43(10)	92.28(11)
D1–Ni–D5	84.58(7)	87.02(7)	–	–
D2–Ni–D3	92.49(8)	93.59(8)	89.43(10)	92.28(11)
D2–Ni–D4	106.68(8)	103.53(8)	180.00(15)	168.16(15)
D2–Ni–D5	107.47(7)	109.64(7)	–	–
D3–Ni–D4	86.02(8)	88.79(8)	90.57(10)	88.83(11)
D3–Ni–D5	91.47(7)	90.88(7)	–	–
D4–Ni–D5	145.82(8)	146.78(8)	–	–

[a] For the numbering scheme see Figure 15.

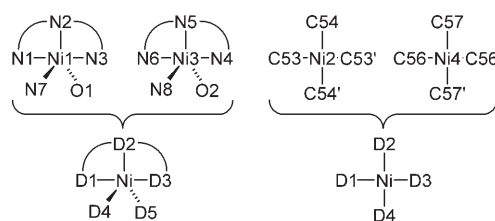


Figure 15. Crystallographic (top) and unified (bottom) numbering scheme used for the complex fragments of $\mathbf{16'}$ in Table 2.

two-dimensional sheet structure is avoided and a tetranodal three-dimensional network is formed instead (Figure 14).

Conclusion

In summary, we have developed a rational synthetic entry to coordination polymers of $\text{Ni}(\text{trpy})$ subunits starting from the examination of simple solvent association processes. Sufficient knowledge was acquired to find appropriate external ligands (donor type, size, charge were factors to consider) for nickeltripyrins so that supramolecular assemblies could be obtained by the associative polymerisation of monomers. Thanks to the very positive crystallisation properties of most of the tripyrrin derivatives we were able to demonstrate the structural variety of accessible topologies. The finding of additional hydrogen bonding and π stacking as well as the production of functionalised inner surfaces further increases the complexity and potential usefulness of the system. $\text{Ni}(\text{trpy})$ fragments can thus be regarded as versatile building blocks for the development of coordination networks and metal organic frameworks (MOFs).

Experimental Section

General: Solvents were dried according to standard procedures and saturated with argon. All reagents were purchased from commercial sources

and used as received unless stated otherwise. Pyrroles **1–3** and tripyrins **4** and **5** were prepared as described previously.^[24] NMR spectra were obtained with a Bruker AMX 400 spectrometer. Chemical shifts (δ) are given in ppm relative to residual protio solvent resonances (¹H NMR spectra) or to chloroform (¹³C NMR spectra). Mass spectra were recorded with a Finnigan 90 MAT (EI, FAB), Finnigan-MAT 95S (ESI) or Bruker Biflex IV instrument (MALDI-TOF). *m/z* values are given for the most abundant isotopes only. UV data were collected with a Shimadzu UV-1601 PC spectrophotometer. FTIR spectra were obtained for samples in Nujol paste with a Bruker Vector 22 instrument.

Isocyanato(2,7,8,13-tetraethyl-1,3,12,14-tetramethyltripyrinato)nickel(II) (6): Tripyrin as bis(hydrotrifluoroacetate) **4** (1.0 mmol) was treated with a solution of Ni(OAc)₂·4H₂O (2.49 g, 10 mmol) and NaOAc (820 mg, 10 mmol) in methanol (15 mL). The resulting green solution was stirred at ambient temperature for 10 min and directly purified by means of chromatography on silica gel with diethyl ether/methanol (4:1) as the eluent. The green-blue fraction was collected, diluted with diethyl ether (500 mL) and washed twice with water (500 mL). A saturated solution of sodium cyanate in water (200 mL) was then added and the mixture vigorously stirred for 5 min. After phase separation the organic layer was dried with sodium sulfate, the solvent evaporated in vacuo and the residue recrystallised from diethyl ether to yield the title compound as violet cubes (210 mg, 43%). ¹H NMR (CD₂Cl₂, 25 °C): δ = 39.5 (brs, 6H; CH₃), 34.3 (brs, 6H; CH₃), 17.9 (brs, 4H; CH₂), 11.2 (brs, 4H; CH₂), 3.8 (brs, 6H; CH₃), 2.9 (brs, 6H; CH₃), 2.2 ppm (brs, 2H; H_{meso}); IR (Nujol): $\tilde{\nu}$ = 2208 (NCO), 1586 cm⁻¹ (C=C); UV/Vis (CH₂Cl₂): λ_{max} (ϵ) = 284 (18000), 353 (54000), 400 (12000), 640sh (24000), 678 nm (34000 mol⁻¹dm³cm⁻¹); MS (70 eV, EI): *m/z*: 488 [M]⁺, 446 [M⁺-NCO]; elemental analysis calcd (%) for C₂₇H₃₄N₄NiO (489.3): C 66.28, H 7.00, N 11.45; found: C 66.04, H 7.01, N 11.27.

Isocyanato(2,3,7,8,9,12,13-hexaethyl-1,14-dimethyltripyrinato)nickel(II) (7): Prepared from tripyrin as the bis(hydrotrifluoroacetate) **5** (1.0 mmol), as described for **6**, yielded **7** as violet crystals (284.5 mg, 55%). ¹H NMR (CD₂Cl₂, 25 °C): δ = 38.5 (brs, 6H; CH₃), 21.5 (brs, 4H; CH₂), 17.8 (brs, 4H; CH₂), 11.2 (brs, 4H; CH₂), 3.7 (brs, 6H; CH₃), 3.6 (brs, 6H; CH₃), 2.7 (brs, 6H; CH₃), 2.0 ppm (brs, 2H; H_{meso}); IR (Nujol): $\tilde{\nu}$ = 2210 (NCO), 1585 cm⁻¹ (C=C); UV/Vis (CH₂Cl₂): λ_{max} (ϵ) = 284 (18000), 353 (54000), 400 (12000), 648sh (26000), 678 nm (34000 mol⁻¹dm³cm⁻¹); MS (70 eV, EI): *m/z*: 516 [M]⁺, 474 [M⁺-NCO]; elemental analysis calcd (%) for C₂₉H₃₈N₄NiO (517.3): C 67.33, H 7.40, N 10.83; found: C 67.23, H 7.27, N 10.79.

Ligand exchange by treatment with aqueous salt solutions—general procedure: A solution of nickeltripyrin complex **6** or **7** (0.1 mmol) in diethyl ether (30 mL) was treated with a saturated NaX or KX solution (15 mL; X = anionic ligand) and stirred vigorously for 16 h. The ether was removed from the mixture in vacuo and the product filtered off and washed with additional water. If the residue was of sufficiently low solubility it was washed with cold pentane or methanol and dried.

Salicylato(2,7,8,13-tetraethyl-1,3,12,14-tetramethyltripyrinato)nickel(II) (8): Prepared from **6** and excess sodium salicylate as a violet solid after crystallisation from dichloromethane/*n*-hexane (44 mg, 76%). ¹H NMR (CD₂Cl₂, 25 °C): δ = 32.8 (brs, 6H; CH₃), 22.4 (brs, 6H; CH₃), 18.4 (brs, 4H; CH₂), 11.0 (brs, 1H; H_A), 9.5 (brs, 4H; CH₂), 7.3 (brs, 1H; H_A), 6.9 (brs, 6H; CH₃), 5.3 (brs, 1H; H_A), 1.0 (brs, 2H; H_{meso}), 0.7 (brs, 6H; CH₃), -2.1 ppm (brs, 1H, H_A); the signal from the OH group could not be detected; IR (Nujol): $\tilde{\nu}$ = 3385 (OH), 1584 cm⁻¹ (C=C, C=O); UV/Vis (CH₂Cl₂): λ_{max} (ϵ) = 284 (15000), 352 (36000), 400 (9000), 640sh (17000), 676 nm (22000 mol⁻¹dm³cm⁻¹); MS (70 eV, EI): *m/z*: 446 [M⁺-sal]; elemental analysis calcd (%) for C₃₃H₃₉N₃NiO₃ (584.4): C 67.83, H 6.73, N 7.19; found: C 67.57, H 6.84, N 7.14.

Cyanido-(2,3,7,8,9,12,13-hexaethyl-1,14-dimethyltripyrinato)nickel(II) (9): Prepared from **7** and sodium cyanide (0.11 mmol, 5.4 mg) as a violet solid (41 mg, 83%). ¹H NMR (CD₂Cl₂, 25 °C): δ = 6.55 (s, 2H; H_{meso}), 2.95 (s, 6H; CH₃), 2.55 (q, ³J(H,H) = 7.6 Hz, 4H; CH₂), 2.46 (q, ³J(H,H) = 7.6 Hz, 4H; CH₂), 2.34 (q, ³J(H,H) = 7.6 Hz, 4H; CH₂), 1.14 (t, ³J(H,H) = 7.6 Hz, 6H; CH₃), 1.10 (t, ³J(H,H) = 7.6 Hz, 6H; CH₃), 1.04 ppm (t, ³J(H,H) = 7.6 Hz, 6H; CH₃); ¹³C NMR (CD₂Cl₂, 25 °C): δ = 177.3, 149.7, 140.5, 140.1, 139.8, 139.5, 118.2, 21.0, 18.4, 18.1, 17.7, 17.2,

16.8, 14.6 ppm; IR (Nujol): $\tilde{\nu}$ = 2117 (CN), 1585 cm⁻¹ (C=C); UV/Vis (CH₂Cl₂): λ_{max} (ϵ) = 288 (18000), 358 (52000), 444sh (9000), 603 (18000), 689 nm (21000 mol⁻¹dm³cm⁻¹); MS (70 eV, EI): *m/z*: 474 [M⁺-CN]; elemental analysis calcd (%) for C₂₉H₃₈N₄Ni (501.3): C 69.47, H 7.64, N 11.17; found: C 69.22, H 7.65, N 11.02.

Isothiocyano(2,3,7,8,9,12,13-hexaethyl-1,14-dimethyltripyrinato)nickel(II) (10): Prepared from **7** and excess potassium thiocyanate as a violet solid (20 mg, 37%). ¹H NMR (CD₂Cl₂, 25 °C): δ = 18.2 (brs, 6H; CH₃), 13.7 (brs, 4H; CH₂), 11.7 (brs, 4H; CH₂), 9.5 (brs, 4H; CH₂), 3.3 (brs, 6H; CH₃), 3.1 (brs, 6H; CH₃), 1.6 (brs, 6H; CH₃), 1.4 ppm (brs, 2H; H_{meso}); IR (Nujol): $\tilde{\nu}$ = 2105 (NCS), 1591 cm⁻¹ (C=C); UV/Vis (CH₂Cl₂): λ_{max} (ϵ) = 280 (10200), 354 (19700), 494 (4300), 654sh (8100), 674 nm (9800 mol⁻¹dm³cm⁻¹); MS (70 eV, EI): *m/z*: 474 [M⁺-NCS]; elemental analysis calcd (%) for C₂₉H₃₈N₄NiS (533.4): C 65.30, H 7.18, N 10.50; found: C 65.23, H 7.22, N 10.48.

Isoselenocyanato(2,3,7,8,9,12,13-hexaethyl-1,14-dimethyltripyrinato)nickel(II) (11): Prepared from **7** and excess potassium selenocyanate as a violet solid (35 mg, 61%). ¹H NMR (CD₂Cl₂, 25 °C): δ = 16.1 (brs, 6H; CH₃), 12.0 (brs, 4H; CH₂), 10.7 (brs, 4H; CH₂), 8.5 (brs, 4H; CH₂), 3.0 (brs, 6H; CH₃), 2.8 (brs, 6H; CH₃), 1.6 (brs, 6H; CH₃), 1.3 ppm (brs, 2H; H_{meso}); IR (Nujol): $\tilde{\nu}$ = 2113 (NCSe), 1591 cm⁻¹ (C=C); UV/Vis (CH₂Cl₂): λ_{max} (ϵ) = 286 (12000), 354 (44000), 400sh (10000), 640sh (20000), 681 nm (27000 mol⁻¹dm³cm⁻¹); MS (70 eV, EI): *m/z*: 474 [M⁺-NCSe]; elemental analysis calcd (%) for C₂₉H₃₈N₄NiSe (580.3): C 60.02, H 6.60, N 9.65; found: C 59.94, H 6.84, N 9.38.

Dinuclear complex (12): Isoselenocyanate **11** was dissolved in dichloromethane, layered with *n*-hexane and kept in a closed vessel at 4 °C for 2 months whereupon violet crystals of **12**·CH₂Cl₂ formed. These crystals were filtered off, washed with cold pentane and dried in air. ¹H NMR (CD₂Cl₂, 25 °C): δ = 17.9 (brs, 4H; CH₂), 11.3 (brs, 4H; CH₂), 8.0 (brs, 4H; CH₂), 5.8 (brs, 2H; H_{meso}), 5.5 (brs, 6H; CH₃), 2.4 (brs, 4H; CH₂), 2.3 (brs, 4H; CH₂), 2.2 (brs, 4H; CH₂), 1.0 (brs, 6H; CH₃), 0.9 (brs, 6H; CH₃), 0.8 (brs, 6H; CH₃), 0.1 (brs, 6H; CH₃), 0.0 (brs, 6H; CH₃), -6.0 ppm (brs, 6H; CH₃); as a result of severe line broadening the signals for one CH₃ group and for one H_{meso} could not be detected unambiguously; IR (Nujol): $\tilde{\nu}$ = 2174, 2153 (CN), 2086 (NCSe), 1597 cm⁻¹ (C=C); UV/Vis (CH₂Cl₂): λ_{max} (ϵ_{rel}) = 283 (0.20), 343sh (0.45), 356 (0.55), 560sh (0.26), 603 (0.43), 679 nm (0.26); MS (70 eV, EI): *m/z*: 474 [Ni⁺(trpy)]; elemental analysis calcd (%) for C₃₈H₇₆N₈Ni₂Se × CH₂Cl₂ (1166.6): C 60.74, H 6.73, N 9.60; found: C 60.52, H 6.71, N 9.69.

Dicyanoamido(2,7,8,13-tetraethyl-1,3,12,14-tetramethyltripyrinato)nickel(II) (13): Prepared from **6** and excess sodium dicyanoamide as a violet solid (39 mg, 75%). ¹H NMR ([D₆]DMSO, 25 °C): δ = 19.2 (brs, 4H; CH₂), 7.9 (brs, 4H; CH₂), 5.0 (brs, 6H; CH₃), 2.1 (brs, 6H; CH₃), 0.4 (brs, 6H; CH₃), -8.9 (brs, 2H; H_{meso}), -12.2 ppm (brs, 6H; CH₃); IR (Nujol): $\tilde{\nu}$ = 2314, 2251, 2185 (CN), 1587 cm⁻¹ (C=C); MS (70 eV, EI): *m/z*: 446 [M⁺-NCNCN]; elemental analysis calcd (%) for C₂₈H₃₄N₆Ni (513.3): C 65.52, H 6.68, N 16.37; found: C 65.34, H 6.84, N 16.38.

Tricyanomethanido(2,7,8,13-tetraethyl-1,3,12,14-tetramethyltripyrinato)nickel(II) (14): Prepared from **6** and excess potassium tricyanomethanide as a violet solid (49 mg, 92%). ¹H NMR ([D₆]DMSO, 25 °C): δ = 19.2 (brs, 4H; CH₂), 7.9 (brs, 4H; CH₂), 5.0 (brs, 6H; CH₃), 2.1 (brs, 6H; CH₃), 0.4 (brs, 6H; CH₃), -8.9 (brs, 2H; H_{meso}), -12.2 ppm (brs, 6H; CH₃); IR (Nujol): $\tilde{\nu}$ = 2233, 2176 (CN), 1586 cm⁻¹ (C=C); MS (70 eV, EI): *m/z*: 446 [M⁺-C(CN)₃]; elemental analysis calcd (%) for C₃₀H₃₄N₆Ni (537.3): C 67.06, H 6.37, N 15.64; found: C 66.92, H 6.37, N 15.59.

Dicyanidoargentato(2,7,8,13-tetraethyl-1,3,12,14-tetramethyltripyrinato)nickel(II) (15): Prepared from **6** and excess sodium dicyanidoargentate as a violet solid (60 mg, 99%). ¹H NMR ([D₆]DMSO, 25 °C): δ = 19.2 (brs, 4H; CH₂), 7.9 (brs, 4H; CH₂), 5.0 (brs, 6H; CH₃), 2.1 (brs, 6H; CH₃), 0.4 (brs, 6H; CH₃), -8.9 (brs, 2H; H_{meso}), -12.2 ppm (brs, 6H; CH₃); IR (Nujol): $\tilde{\nu}$ = 2172 (CN), 1598 cm⁻¹ (C=C); MS (70 eV, EI): *m/z*: 446 [M⁺-Ag(CN)₂]; elemental analysis calcd (%) for C₂₈H₃₄AgN₅Ni (607.2): C 55.39, H 5.64, N 11.53; found: C 55.58, H 5.48, N 11.35.

Tetracyanidoniccolatobis[(2,7,8,13-tetraethyl-1,3,12,14-tetramethyltripyrinato)nickel(II)] (16): Prepared from **6** and excess dipotassium tetracyanidoniccolate as a violet solid (60 mg, 83%). ¹H NMR ([D₆]DMSO,

25°C): $\delta = 19.2$ (brs, 4H; CH₂), 7.9 (brs, 4H; CH₂), 5.0 (brs, 6H; CH₃), 2.1 (brs, 6H; CH₃), 0.4 (brs, 6H; CH₃), -8.9 (brs, 2H; H_{meso}), -12.2 ppm (brs, 6H; CH₃); IR (Nujol): $\tilde{\nu} = 2155$ (CN), 1600 cm⁻¹ (C=C); MS (70 eV, EI): m/z : 446 [Ni⁺(trpy)]; elemental analysis calcd (%) for C₅₆H₆₈N₁₀Ni₃ (1057.3): C 63.62, H 6.48, N 13.25; found: C 63.40, H 6.68, N 12.99.

X-ray crystallographic study of 7–10, 12–14 and 16': Suitable crystals of the complexes **7–10**, **12–14** and **16'** were obtained by layering concentrated solutions of the compounds in dichloromethane or methanol with *n*-hexane or toluene and allowing slow diffusion below room temperature. Crystal data and experimental details are given in Table 1.

CCDC-619880 to CCDC-619887 contain the supplementary crystallographic data for this paper. These data can be obtained free of charge from the Cambridge Crystallographic Data Centre via www.ccdc.cam.ac.uk/data_request/cif.

Acknowledgements

We gratefully acknowledge financial support from the Deutsche Forschungsgemeinschaft (DFG).

- [1] S. R. Batten, R. Robson, *Angew. Chem.* **1998**, *110*, 1558–1595; *Angew. Chem. Int. Ed.* **1998**, *37*, 1460–1494.
- [2] C. Janiak, *J. Chem. Soc., Dalton Trans.* **2003**, 2781–2804.
- [3] S. R. Batten, K. S. Murray, *Coord. Chem. Rev.* **2003**, *246*, 103–130.
- [4] A. Erxleben, *Coord. Chem. Rev.* **2003**, *246*, 203–228.
- [5] G. K. H. Shimizu, *J. Solid State Chem.* **2005**, *178*, 2519–2526.
- [6] a) G. Férey, M. Latroche, C. Serre, F. Millange, T. Loiseau, A. Percheron-Guégan, *Chem. Commun.* **2003**, 2976–2977; b) J. L. C. Rowsell, A. R. Millward, K. S. Park, O. M. Yaghi, *J. Am. Chem. Soc.* **2004**, *126*, 5666–5667; c) J. L. C. Rowsell, O. M. Yaghi, *Angew. Chem.* **2005**, *117*, 4748–4758; *Angew. Chem. Int. Ed.* **2005**, *44*, 4670–4679; d) P. Horcajada, C. Serre, M. Vallet-Regí, M. Sebban, F. Tauler, G. Férey, *Angew. Chem.* **2006**, *118*, 6120–6124; *Angew. Chem. Int. Ed.* **2006**, *45*, 5974–5978.
- [7] D. Braga, *J. Chem. Soc., Dalton Trans.* **2000**, 3705–3714.
- [8] M. J. Zaworotko, *Chem. Commun.* **2001**, 1–10.
- [9] B. Moulton, M. J. Zaworotko, *Chem. Rev.* **2001**, *101*, 1629–1658.
- [10] M. W. Hosseini, *Coord. Chem. Rev.* **2003**, *240*, 157–166.
- [11] A. M. Beatty, *Coord. Chem. Rev.* **2003**, *246*, 131–143.
- [12] S. P. Rath, M. M. Olmstead, L. Latos-Grażyński, A. L. Balch, *J. Am. Chem. Soc.* **2003**, *125*, 12678–12679.
- [13] A. Krivokapic, A. R. Cowley, H. L. Anderson, *J. Org. Chem.* **2003**, *68*, 1089–1096.
- [14] H. Furuta, H. Maeda, A. Osuka, *Inorg. Chem. Commun.* **2003**, *6*, 162–164.
- [15] J. L. Sessler, A. Gebauer, V. Král, V. Lynch, *Inorg. Chem.* **1996**, *35*, 6636–6637.
- [16] A. Jaumà, J.-A. Farrera, J. M. Ribó, *Monatsh. Chem.* **1996**, *127*, 935–946.
- [17] R. G. Khoury, M. O. Senge, J. E. Colchester, K. M. Smith, *J. Chem. Soc., Dalton Trans.* **1996**, 3937–3950.
- [18] D. Eichinger, H. Falk, *Monatsh. Chem.* **1987**, *118*, 261–271.
- [19] F.-P. Montforts, U. M. Schwartz, *Liebigs Ann. Chem.* **1985**, 1228–1253.
- [20] F.-P. Montforts, *Angew. Chem.* **1981**, *93*, 795–796; *Angew. Chem. Int. Ed. Engl.* **1981**, *20*, 778–779.
- [21] H. von Dobeneck, U. Sommer, E. Brunner, E. Lippacher, F. Schnerle, *Justus Liebigs Ann. Chem.* **1973**, *11*, 1934–1942.
- [22] M. Bröring, C. D. Brandt, *Chem. Commun.* **2001**, 499–500.
- [23] M. Bröring, C. D. Brandt, *J. Chem. Soc., Dalton Trans.* **2002**, 1391–1395.
- [24] M. Bröring, C. D. Brandt, S. Prikhodovski, *J. Porphyrins Phthalocyanines* **2003**, *7*, 17–24.
- [25] A. Srinivasan, H. Furuta, *Acc. Chem. Res.* **2005**, *38*, 10–20.
- [26] M. Stępień, L. Latos-Grażyński, *Acc. Chem. Res.* **2005**, *38*, 88–98.
- [27] L. Latos-Grażyński in *The Porphyrin Handbook, Vol. 1* (Eds.: K. M. Kadish, K. M. Smith, R. Guilard), Academic Press, New York, **2000**, pp. 361–416.
- [28] M. Bröring, S. Prikhodovski, C. D. Brandt, *J. Chem. Soc., Dalton Trans.* **2002**, 4213–4218.
- [29] M. Bröring, S. Prikhodovski, C. D. Brandt, *Inorg. Chim. Acta* **2004**, *357*, 1733–1738.
- [30] H. Falk, *The Chemistry of Linear Oligopyrroles and Bile Pigments*, Springer, Vienna, **1989**.
- [31] D. F. Evans, *J. Chem. Soc.* **1959**, 2003–2005.
- [32] C. Piguet, *J. Chem. Educ.* **1997**, *74*, 815–816.
- [33] L. Sacconi, F. Mani, A. Bencini in *Comprehensive Coordination Chemistry, Vol. 5* (Ed.: G. Wilkinson), Pergamon, Oxford, **1987**, pp. 1–347.
- [34] a) T. Rojo, R. Cortés, L. Lezama, M. I. Arriortua, K. Urriaga, G. Villeneuve, *J. Chem. Soc., Dalton Trans.* **1991**, 1779–1783; b) R. Vicente, A. Escuer, J. Ribas, X. Solans, *J. Chem. Soc., Dalton Trans.* **1994**, 259–262; c) A. Escuer, R. Vicente, M. S. El Fallah, X. Solans, M. Font-Bardía, *J. Chem. Soc., Dalton Trans.* **1996**, 1013–1019; d) M. Monfort, C. Bastos, C. Dias, J. Ribas, *Inorg. Chim. Acta* **1994**, *218*, 185–188; e) H. Grove, M. Julve, F. Lloret, P. E. Kruger, K. W. Törnroos, J. Sletten, *Inorg. Chim. Acta* **2001**, *325*, 115–124; f) T. K. Maji, I. R. Laskar, G. Mostafa, A. J. Welch, P. S. Mukherjee, N. R. Chaudhuri, *Polyhedron* **2001**, *20*, 651–655; L. Shen, Y.-Z. Xu, *J. Chem. Soc., Dalton Trans.* **2001**, 3413–3414; g) R. Sekiya, S. Nishikiori, *Chem. Eur. J.* **2002**, *8*, 4803–4810; h) A. Skorupa, B. Korybut-Daszkiewicz, J. Mroziński, *Inorg. Chim. Acta* **2002**, *336*, 65–70; i) B. Żurawska, J. Mroziński, M. Julve, F. Lloret, A. Maslejova, W. Sawka-Dobrowolska, *Inorg. Chem.* **2002**, *41*, 1771–1777; j) J. Tercero, C. Diaz, J. Ribas, E. Ruiz, J. Mahía, M. Maestro, *Inorg. Chim. Acta* **2002**, *41*, 6780–6789; k) J. A. Real, A. B. Gaspar, V. Niel, M. C. Muñoz, *Coord. Chem. Rev.* **2003**, *236*, 121–141; l) S. Deoghoría, S. Sain, B. Moulton, M. J. Zaworotko, S. K. Bera, S. K. Chandra, *Polyhedron* **2002**, *21*, 2457–2461.
- [35] a) J. Ribas, C. Diaz, X. Solans, M. Font-Bardía, *J. Chem. Soc., Dalton Trans.* **1996**, 35–38; b) P. M. Secondo, J. M. Land, R. G. Baughman, H. L. Collier, *Inorg. Chim. Acta* **2000**, *309*, 13–22; c) J. Tercero, C. Diaz, J. Ribas, J. Mahía, M. Maestro, X. Solans, *J. Chem. Soc., Dalton Trans.* **2002**, 2040–2046; d) A. B. Gaspar, M. C. Muñoz, N. Moliner, V. Ksenofontov, G. Levchenko, P. Gütllich, J. A. Real, *Monatsh. Chem.* **2003**, *134*, 285–294.
- [36] a) U. Turpeinen, *Finn. Chem. Lett.* **1977**, *6*, 75–78; b) S. Sain, T. K. Maji, G. Mostafa, T.-H. Lu, M. Y. Chiang, N. R. Chaudhuri, *Polyhedron* **2002**, 2293–2299.
- [37] K. Nakamoto, *Infrared and Raman Spectra of Inorganic and Coordination Compounds, Part B, Vol. 5*, Wiley, New York, **1997**, pp. 105–126.
- [38] R. D. Willet, Z. Wang, S. Molnar, K. Brewer, C. P. Landee, M. M. Turnbull, W. Zhang, *Mol. Cryst. Liq. Cryst. Technol., Sect. A* **1993**, *233*, 277–282.
- [39] S. Trofimenko, E. L. Little, Jr., H. F. Mower, *J. Org. Chem.* **1962**, *27*, 433–438.
- [40] For a recent report on hybrid three-dimensional coordination polymers using hydrogen bonds, see: J. Lefebvre, F. Callaghan, M. J. Katz, J. E. Sonier, D. B. Leznoff, *Chem. Eur. J.* **2006**, *12*, 6748–6761.
- [41] SHELXS-97, Program for Crystal Structure Determination, G. M. Sheldrick, University of Göttingen, Göttingen, **1997**.
- [42] SHELXL-97, Program for Crystal Structure Refinement, G. M. Sheldrick, University of Göttingen, Göttingen, **1997**.

Received: September 8, 2006
Published online: November 30, 2006